



# Differential diagnostic value of tumor morphology, long/short diameter ratio, and ultrasound gray-scale ratio for 3 parotid neoplasms

Feifei Xia, SM,<sup>a</sup> Wenjuan Qin, SM,<sup>b</sup> Jia Feng, SM,<sup>b</sup> Xuyang Zhou, SM,<sup>c</sup> Ercan Sun, SM,<sup>a</sup> Jiang Xu, SM,<sup>a</sup> and Changxue Li, SM<sup>a</sup>

**Objective.** The objective of this study was to evaluate the value of tumor morphology, long-to-short diameter ratio (L/S), and ultrasound gray-scale ratio (UGSR) in the differential diagnosis of 3 parotid neoplasms.

**Study Design.** Preoperative ultrasound images of 17 patients with a malignant tumor (MT), 48 patients with pleomorphic adenoma (PA), and 39 patients with adenolymphoma (AL) were analyzed for imaging features and gray-scale histograms. Tumor morphology, L/S, and UGSR of MT, PA, and AL were compared. Receiver operating characteristic analysis of area under the curve (AUC), sensitivity, and specificity were used to measure the differential diagnostic efficacy of L/S, UGSR, and both combined with tumor morphology.

**Results.** Morphologic features, L/S, and UGSR differed significantly in various pairwise comparisons of the 3 tumor types. Acceptable discrimination was detected between MT and AL with UGSR alone (AUC = 0.771) and between PA and AL with L/S and UGSR combined (AUC = 0.741). The combination of tumor boundary with UGSR yielded excellent discrimination between MT and PA (AUC = 0.853) and between MT and AL (AUC = 0.885), with sensitivity and specificity values greater than 0.800.

**Conclusions.** These ultrasound parameters, alone or in combination, can provide a method for accurate presurgical differential diagnosis of parotid tumors. (Oral Surg Oral Med Oral Pathol Oral Radiol 2022;134:484–491)

Parotid gland tumors account for 3% of head and neck neoplasms, of which approximately 20% are malignant tumors (MT) and 80% are benign. Pleomorphic adenoma (PA) is the most common benign tumor, followed by adenolymphoma (AL).<sup>1-3</sup> The clinical manifestations of malignant and benign tumors of the parotid gland are similar, but the surgical treatment and postoperative outcomes are quite different, so it is important to differentiate malignant from benign lesions and distinguish different histologic types before surgery.<sup>4</sup>

Ultrasonography (US) is considered the first-line diagnostic imaging method to assess lymph nodes and soft tissue lesions of the head and neck region, including tumors in the salivary glands.<sup>5-6</sup> Consequently, numerous studies have focused on the differential diagnosis of parotid neoplasms by US.<sup>3-8</sup> These lesions have different properties and morphologic features. Unfortunately, there is a substantial overlap between them, so the differential diagnosis on the basis of US

has always been inadequate. Moreover, interpretation of US findings is mainly dependent on subjective, naked-eye judgment and the clinical experience of an ultrasonographer rather than measurable evidence, leading to unsatisfying results.

A degree of objectivity in the US interpretation of parotid tumors can be provided by 2 parameters: measurement of the ratio of the long diameter of the tumor to the short diameter (L/S) and the ultrasound gray-scale ratio (UGSR), defined as the ratio of the gray-scale of the parotid neoplasm to the surrounding normal parotid tissues under the same operating conditions.<sup>7</sup> L/S does not depend on the skills of the ultrasonographer or the sensitivity or quality of the US machine. It is a quantitative means of assessing tumor shape, related to the texture and elasticity of the solid tumor to some extent, and can be easily obtained. L/S has been shown to be helpful in the differential diagnosis of PA and AL.<sup>8</sup>

UGSR is valuable because there is a strong correlation between the intensity of echogenicity and the gray scale of the ultrasound image.<sup>9</sup> The intensity is shown in a black-to-white gray scale, reflecting differences between nodules and surrounding tissues. However,

<sup>a</sup>Department of Stomatology, First Affiliated Hospital of Shihezi University School of Medicine, China.

<sup>b</sup>Department of Ultrasound, First Affiliated Hospital of Shihezi University School of Medicine, China.

<sup>c</sup>Department of Pathology, First Affiliated Hospital, Shihezi University School of Medicine, China.

Corresponding author: Changxue Li. E-mail address: 3541226598@qq.com

Received for publication Nov 22, 2021; returned for revision May 19, 2022; accepted for publication May 25, 2022.

© 2022 The Author(s). Published by Elsevier Inc. This is an open access article under the CC BY-NC-ND license (<http://creativecommons.org/licenses/by-nc-nd/4.0/>)

2212-4403/\$-see front matter

<https://doi.org/10.1016/j.oooo.2022.05.012>

## Statement of Clinical Relevance

The parameters of tumor boundary, long/short diameter ratio, and ultrasound gray-scale ratio, alone or combined, provide acceptable to excellent presurgical discrimination between malignant tumors, pleomorphic adenoma, and adenolymphoma in the parotid gland.

the gray scale is also affected by other factors, such as gain level, dynamic range, and frequency. Therefore, there is no applicable method for gray-scale level measurement of all ultrasonic images. However, no matter how the gray-scale level changes in parotid neoplasms, there is still a “low” and “high” relative ratio between gray-scale levels of nodules and the surrounding parotid tissue. Studies have shown that UGSR has a certain value in the differential diagnosis of thyroid and breast diseases.<sup>8-10</sup>

Research indicates that there are differences between benign and malignant tumors and between benign tumors of different histologic types regarding texture, elasticity, and the mean gray levels of ultrasonic images.<sup>3,4,7,8</sup> We predicted that tumor morphology, L/S, and UGSR would differ among MT, PA, and AL. Therefore, the objective of this study was to compare the tumor morphologic parameters of boundary, shape, echotexture, anechoic area, and high rear echo; the L/S ratio; and UGSR of MT, PA, and AL in the parotid glands. We hypothesized that these parameters, considered separately or in combination, would differ significantly between the tumors, thereby aiding in the formulation of differential diagnoses.

**MATERIALS AND METHODS**

**Patient Selection**

In this retrospective analysis, 243 consecutive patients with parotid neoplasms treated in the First Affiliated Hospital of the Medical College of Shihezi University from January 2014 to November 2020 were initially included. We excluded 59 patients because of controversial pathologic diagnosis, leaving 184 patients who were diagnosed with MT, PA, or AL in the parotid gland. Next, 47 patients with no preoperative parotid ultrasound examination were excluded, resulting in 137 patients. Finally, 33 patients were excluded because of unclear or incomplete US images. In total, 104 patients were included in the study (Figure 1). There were 17 patients (11 males and 6 females) in the MT group, 48 patients (23 males and 25 females) in PA group, and 39 patients (38 males and 1 female) in AL group. The research was approved by the ethics committee of the First Affiliated Hospital of the Medical College. Written informed consent was waived owing to the noninterventional and retrospective nature of this study.

**US examination**

The Philips EPIQ5 color Doppler ultrasonography unit (Philips Medical Systems, Amsterdam, Netherlands) was used with a probe frequency of 7 to 15 MHz. The patients were positioned to fully expose the parotid region. After smearing an appropriate amount of coupling agent, the probe was placed perpendicular to the

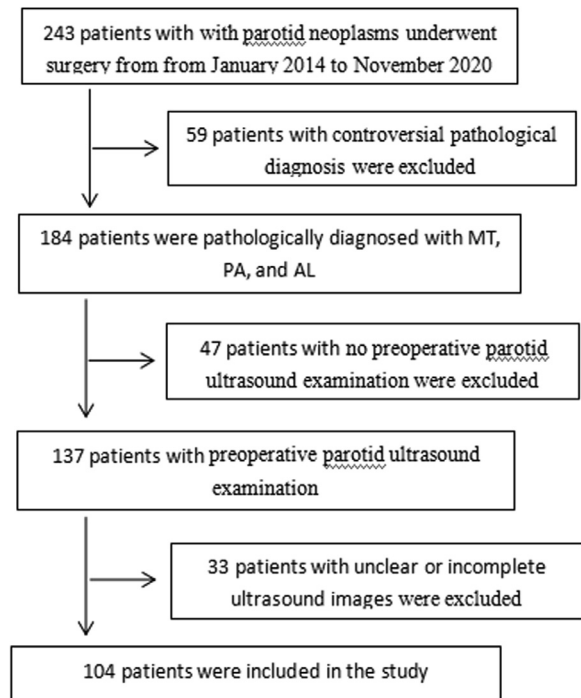


Fig. 1. The recruitment pathway of patients in this study. MT, malignant tumor; PA, pleomorphic adenoma; AL, adenolymphoma.

scan surface with minimal pressure applied to the face, and longitudinal (vertical) ultrasound scans were performed on the parotid glands. The lesions were localized, and the ultrasonographic features of each tumor were observed, including boundary, shape, echotexture, anechoic areas, high rear echo, and the long and short diameters to allow calculation of the L/S diameter ratio. The images were saved in the original data of the Digital Imaging and Communications in Medicine format.

**Image acquisition and analysis**

US data selected from the picture archiving and communication systems (PACS) were independently analyzed by a physician who was experienced in US diagnosis and a chief physician in oral and maxillofacial surgery. Both examiners were blinded to the pathologic diagnoses of the tumors.

The following ultrasound image features of tumor morphology in the 104 lesions were analyzed:

- 1 Boundary, classified as clear (with complete capsule echo) or unclear (blurred with surrounding parotid tissue, no obvious capsule echo).
- 2 Shape, classified as regular (round or oval) or irregular (lobulated edge or “burr sign”).
- 3 Echotexture, characterized as homogeneous (when the tumor contained echolucent areas only) or heterogeneous (when the lesion contained echolucent

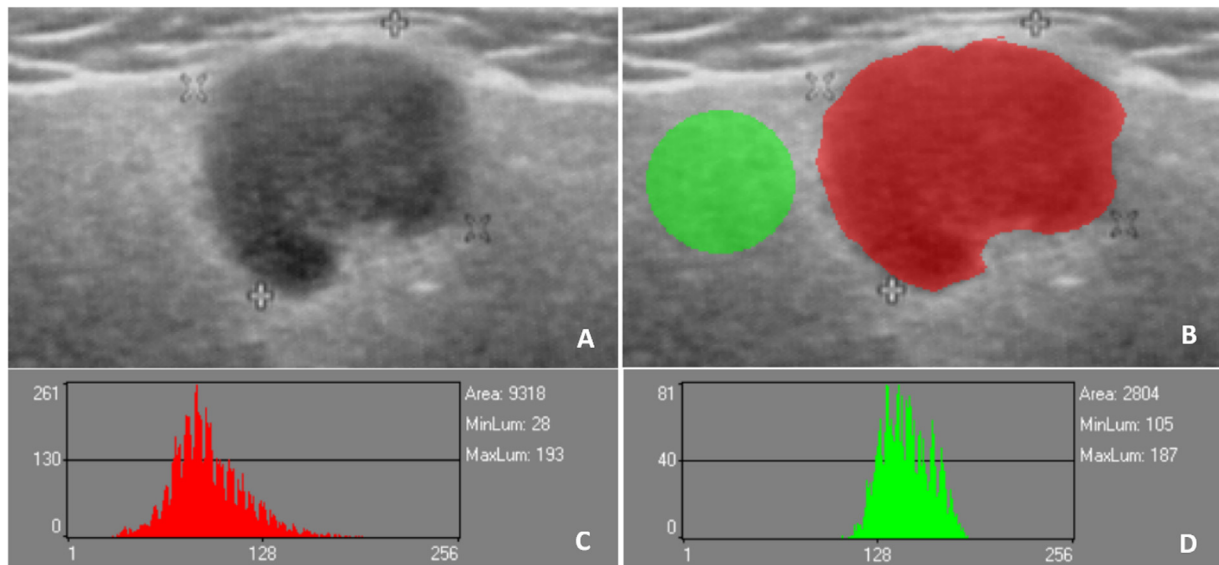


Fig. 2. A 48-year-old woman with an MT (acinar cell carcinoma) in the right parotid gland. (A) A homogeneous hypoechoic mass with a clear boundary and irregular shape was detected by gray-scale ultrasonography. Anechoic areas were not observed. A high rear echo was detected. The long diameter and short diameter were 1.41 and 1.35 cm, respectively, with a long-to-short diameter ratio of 1.04. (B) A region of interest (ROI) was drawn along the edge of the parotid tumor and marked with red filling. A round ROI was selected in the normal parotid tissue image area around the lesion and filled with green. (C) The software automatically generated gray histogram and gray characteristic parameters including the average gray values of the parotid neoplasm and the surrounding normal parotid tissues. Based on the histogram of the tumor ROI, the mean value of the gray scale was 120.70. (D) The ROI histogram of the normal parotid tissues had a mean gray value of 166.34.

areas and distinct areas of clearly increased or decreased echogenicity).

- 4 Anechoic areas, characterized by the presence of cystic components that appeared anechoic.
- 5 High rear echo, characterized by the presence of echolucent areas that were significantly increased below the tumor region.
- 6 Long diameter (the longest axis of the tumor) and short diameter (the anteroposterior diameter perpendicular to the long diameter), measured in cm, which were used to calculate L/S.

Data regarding the categorical image features of boundary, shape, echotexture, anechoic areas, and high rear echo were entered independently by the 2 physicians. In cases of disagreement, consensus was reached by discussion. The 2 physicians independently measured the long and short diameters of each tumor, from which L/S was calculated. The mean values of their measurements were used for statistical analysis.

After downloading the images through PACS, the 2 physicians used Mazda 4.6 software<sup>11</sup> (<http://www.elte.p.lodz.pl/mzada/>) together to complete the gray histogram texture analysis. A region of interest (ROI) was drawn along the edge of the parotid tumor and marked with red filling. A round ROI was selected in the normal parotid tissue image area around the lesion and filled with green, and the software automatically

generated gray histogram and gray characteristic parameters including the average gray values of the parotid neoplasm and the surrounding normal parotid tissues. Examples are shown in Figures 2, 3, and 4. Finally, the UGSR was calculated.

**Statistical analysis**

SPSS 22.0 (SPSS Inc., Chicago, IL, USA) was used for statistical analysis of the data. The chi-square test was employed to compare the differences of boundary, shape, echotexture, and anechoic areas among MT, PA, and AL, and for pairwise comparisons of MT vs PA, MT vs AL, and PA vs AL. Due to the small numbers of expected frequencies in some cells, the Fisher exact test was used to compare the differences in high rear echo among PA and AL. The alpha level for significance was established at  $P < .05$  for overall comparisons among the tumor groups but was lowered from .05 to .017 using the Bonferroni correction for pairwise comparisons.

All numeric data were reported as mean  $\pm$  standard deviation (SD) in cm. Since measurements of the short diameter had a normal distribution, the  $t$  test was used for comparisons of this parameter among MT, PA, and AL. The long diameter, L/S, and UGSR values were non-normally distributed and were analyzed with the Kruskal-Wallis (K samples) test. SPSS 22.0 was used to generate the receiver operating characteristic

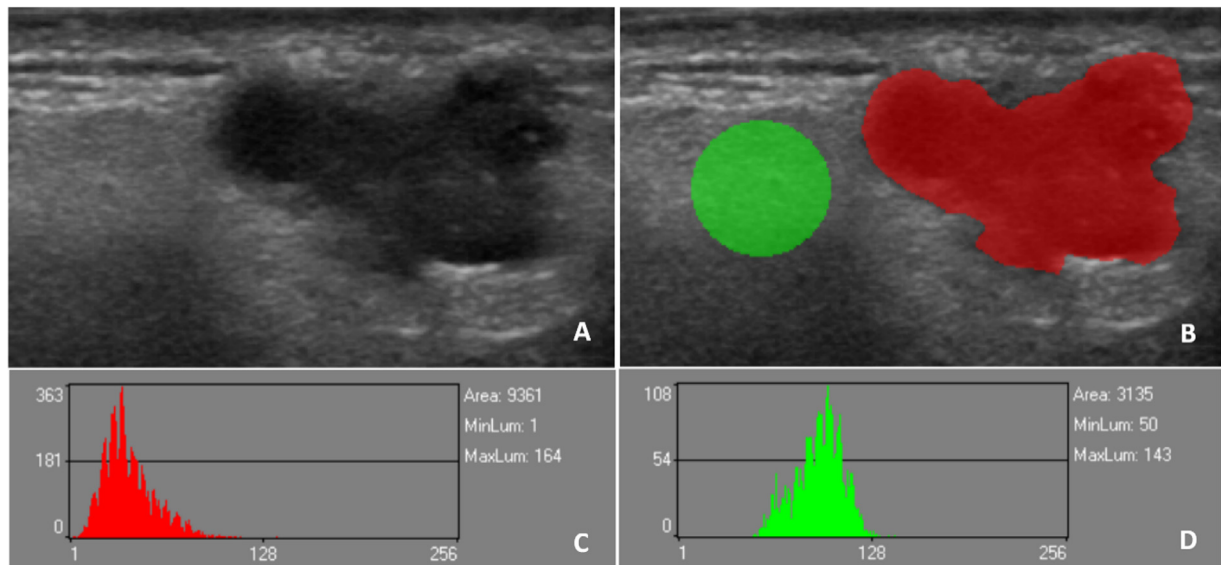


Fig. 3. A 46-year-old woman with a PA in the right parotid gland. **(A)** A heterogeneous hypoechoic mass with an unclear boundary and irregular shape was detected by gray-scale ultrasonography. Anechoic areas were not observed. A high rear echo was observed. The long diameter and short diameter were 2.33 and 1.41 cm, respectively, with a long-to-short diameter ratio of 1.65. **(B)** A region of interest (ROI) was drawn along the edge of the parotid tumor and marked with red filling. A round ROI was selected in the normal parotid tissue image area around the lesion and filled with green. **(C)** The software automatically generated gray histogram and gray characteristic parameters including the average gray values of the parotid neoplasm and the surrounding normal parotid tissues. Based on the histogram of the tumor ROI, the mean value of the gray scale was 45.41. **(D)** The ROI histogram of the normal parotid tissues had a mean gray value of 114.20.

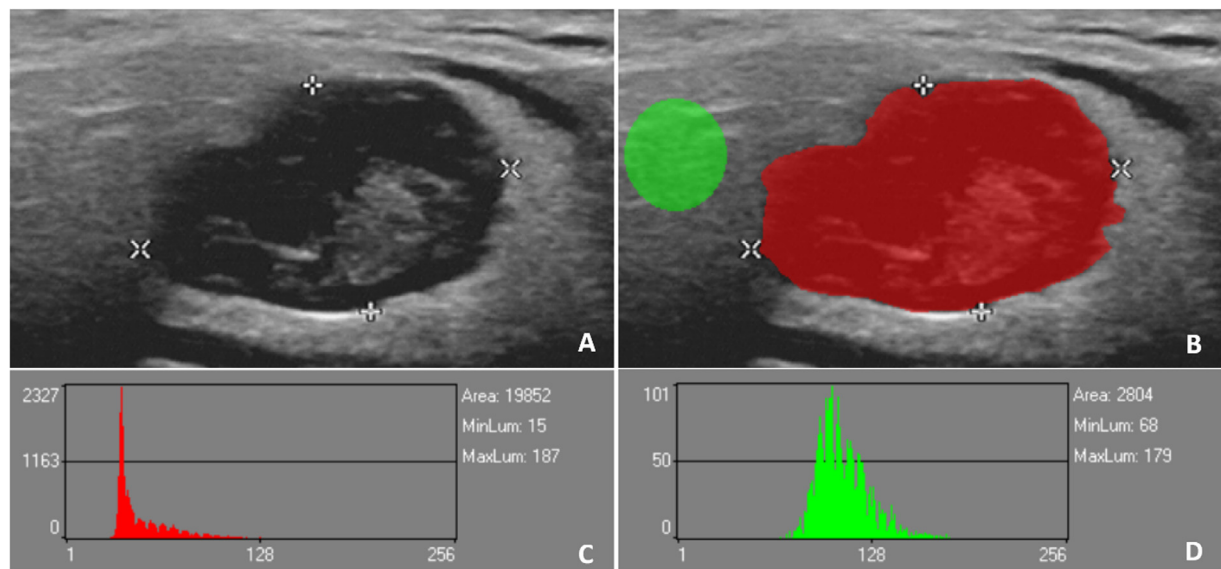


Fig. 4. A 60-year-old man with an AL in the right parotid gland. **(A)** A heterogeneous hypoechoic mass with a clear boundary and irregular shape was detected by gray-scale ultrasonography. Anechoic areas and high rear echo were observed. The long diameter and short diameter were 2.09 and 0.97 cm, respectively, with a long-to-short diameter ratio of 2.15. **(B)** A region of interest (ROI) was drawn along the edge of the parotid tumor and marked with red filling. A round ROI was selected in the normal parotid tissue image area around the lesion and filled with green. **(C)** The software automatically generated gray histogram and gray characteristic parameters including the average gray values of the parotid neoplasm and the surrounding normal parotid tissues. Based on the histogram of the tumor ROI, the mean value of the gray scale was 53.39. **(D)** The ROI histogram of the normal parotid tissues had a mean gray value of 134.47.

(ROC) curve, with sensitivity as the ordinate and 1-specificity as the abscissa. On this curve, the closer the point was to the upper-left corner, the higher the sensitivity and specificity. The point that was the closest to the upper-left corner represented the best cutoff value to maximize sensitivity and specificity. The area under the ROC curve (AUC) was calculated to estimate the overall accuracy of the parameters. Diagnostic performance was calculated using the cutoff values according to the Youden index, which is defined as the maximum of *sensitivity + specificity - 1* over all possible decision thresholds. *P* < .05 was considered statistically significant.

**RESULTS**

**Comparison of tumor morphology**

Overall comparisons revealed significant differences in boundary, shape, high rear echo, long diameter, and short diameter among groups (*P* ≤ .016). Pairwise comparisons discovered which specific groups were significantly different. The boundary of MT was more unclear than that of PA and AL (*P* < .001), but there was no significant difference between PA and AL (*P* = .736). The shape of MT was more irregular than that of AL (*P* = .007), but there was no significant difference between MT and PA or between PA and AL (*P* ≥ .050). High rear echo was less common in MT than in PA (*P* = .001), but there was no significant

difference between MT and AL or between PA and AL (*P* ≥ .040). The long diameter of AL was significantly greater than that of MT (*P* = .001). The short diameter of AL was significantly longer than the short diameter of MT (*P* = .006) and PA (*P* = .005). No significant differences were discovered among the tumor groups regarding echotexture or the presence of anechoic areas (*P* ≥ .273). All data are listed in [Table I](#).

**Comparison of L/S and UGSR**

Overall comparisons revealed significant differences in L/S and UGSR among groups (*P* ≤ .010). Pairwise comparisons discovered which specific groups were significantly different. The average L/S values of MT, PA, and AL were 1.604 ± 0.331, 1.443 ± 0.230, and 1.633 ± 0.335, respectively. Pairwise comparisons showed that the L/S value of AL was higher than that of PA, and the difference approached significance (*P* = .018). There was no significant difference between the L/S values of MT and PA (*P* = .101) or AL (*P* = .824). The average UGSR values of MT, PA, and AL were 0.519 ± 0.151, 0.429 ± 0.152, and 0.359 ± 0.141, respectively. Pairwise comparison between the 3 groups revealed that the UGSR value of MT was significantly higher than that of PA (*P* = .002) and AL (*P* = .001), but the difference between PA and AL (*P* = .029) was not significant ([Table II](#)).

**Table I.** Tumor morphology of MT, PA, and AL

Parameters	Tumor classification			Among groups P value	Comparison between groups	Pairwise comparison P value
	MT (1)	PA (2)	AL (3)			
<i>Boundary</i>				< .001*	1 VS 2 1 VS 3 2 VS 3	< .001* < .001* .736
Clear	3 (17.6)	38 (79.2)	32 (82.1)			
Unclear	14 (82.4)	10 (20.8)	7 (17.9)			
<i>Shape</i>				.016*	1 VS 2 1 VS 3 2 VS 3	.173 .007* .050
Regular	3 (17.6)	17 (35.4)	22 (56.4)			
Irregular	14 (82.4)	31 (64.6)	17 (43.6)			
<i>Echotexture</i>				.477	1 VS 2 1 VS 3 2 VS 3	.446 .383 .836
Homogeneous	3 (17.6)	15 (31.2)	13 (33.3)			
Heterogeneous	14 (82.4)	33 (68.8)	26 (66.7)			
<i>Anechoic areas</i>				.273	1 VS 2 1 VS 3 2 VS 3	.522 .562 .107
Yes	6 (35.3)	13 (27.1)	17 (43.6)			
No	11 (64.7)	35 (72.9)	22 (56.4)			
<i>High rear echo</i>				.005*	1 VS 2 1 VS 3 2 VS 3	.001* .157 .040
Yes	11 (64.7)	46 (95.8)	32 (82.1)			
No	6 (35.3)	2 (4.2)	7 (17.9)			
<i>Long diameter</i>	1.150 ± 0.642	1.626 ± 0.630	1.921 ± 0.669	.001*	1 VS 2 1 VS 3 2 VS 3	.045 .001* .131
<i>Short diameter</i>	2.191 ± 1.157	2.370 ± 0.996	3.016 ± 0.869			
			.002*			

*n*, number of cases; *MT*, malignant tumor; *PA*, pleomorphic adenoma; *AL*, adenolymphoma.

\*Statistically significant difference: *P* < .05 for comparisons among groups, *P* < .017 for pairwise comparisons, Tumor classification for categorical parameters reported as number (%). Tumor classification for numerical parameters reported as mean ± standard deviation in cm.

**Table II.** L/S and UGSR of MT, PA, and AL

Parameters	Tumor classification			Among groups P value	Comparison between groups	Pairwise comparison P value
	MT (1)	PA (2)	AL (3)			
L/S	1.604 ± 0.331	1.443 ± 0.230	1.663 ± 0.335	.010*	1 VS 2 1 VS 3 2 VS 3	.101 .824 .018
UGSR	0.519 ± 0.151	0.429 ± 0.152	0.359 ± 0.141	< .001*	1 VS 2 1 VS 3 2 VS 3	.002* .001* .029

MT, malignant tumor; PA, pleomorphic adenoma; AL, adenolymphoma; L/S, ratio of the long diameter to the short diameter; UGSR, ultrasound gray-scale ratio.

\*Statistically significant difference. *P* < .05 for comparisons among groups, *P* < .017 for pairwise comparisons.

**ROC analysis**

For L/S, the AUC, sensitivity, specificity, Youden index, and optimal cutoff value for distinguishing PA from AL were 0.698, 0.872, 0.500, 0.372, and 1.406, respectively. For UGSR, the AUC, sensitivity, specificity, Youden index, and optimal cutoff value for distinguishing MT from AL were 0.771, 0.824, 0.641, 0.465, and 0.404, respectively. For the combination of L/S and UGSR in the diagnosis of PA and AL, the AUC, sensitivity, specificity, Youden index, and optimal cutoff value were 0.741, 0.744, 0.687, 0.431, and 0.409, respectively. However, the diagnostic efficacy of tumor boundary features combined with UGSR in the differential diagnosis of MT and PA as well as MT and AL were generally better, with AUC, sensitivity, and specificity values all exceeding 0.800, as shown in Table III.

**DISCUSSION**

Although 80% of parotid tumors occur in the superficial lobe of the parotid gland, and surgical resection is the most common management, the treatment of benign and malignant tumors is completely different. Malignant tumors often need radical resection, whereas benign lesions can be treated with modified or functional parotidectomy. In addition, the postoperative recurrence rates of benign tumors vary among different histologic types. Therefore, the preoperative discrimination of benign vs malignant parotid neoplasms and between the histologically different benign lesions is

very important for perioperative preparation, selection of surgical treatment, and communication about the disease.<sup>4,12,13</sup>

Studies have shown that sensitivity and specificity of US features in distinguishing benign and malignant tumors of the parotid gland range from 46.2% to 84% and from 88% to 98%, respectively. The sensitivity and specificity in discriminating between PA and AL have been reported to range from 57% to 96% and 55% to 82% in 2 studies.<sup>4,14</sup> US of MT has revealed unclear edges, irregular shapes, and uneven echo of structure.<sup>7</sup> PA appears as a hypochoic mass with a clear boundary, lobulated shape, and uniform internal echo with posterior enhanced echo, whereas AL often is a hypochoic lesion with a clear boundary, regular round or oval shape, a solid or partially cystic structure, and inhomogeneous internal echoes.<sup>15</sup> In the present study, statistically significant differences were revealed in boundary, shape, and long and short diameters among and between groups; however, there were no significant differences in echotexture or anechoic areas among groups, consistent with other research.<sup>16,17</sup>

The use of these US features to distinguish common parotid tumors depends on the subjective judgment of the radiologists in imaging diagnostics.<sup>15</sup> Lack of objectivity can be addressed with quantitative measures such as L/S ratio, one of the most basic characteristics of tumors that has been widely used to evaluate lymph node diseases.<sup>18</sup> The UGSR value, although acquired with different time compensation gain,

**Table III.** ROC analysis of solitary and multiple parameters to diagnose MT, PA, and AL

Parameters	Tumor group	AUC	Sensitivity	Specificity	Youden index	Optimal cutoff value
L/S	PA, AL	0.698	0.872	0.500	0.372	1.406
USGR	MT, AL	0.771	0.824	0.641	0.465	0.404
L/S + UGSR	PA, AL	0.741	0.744	0.687	0.431	0.409
Boundary + UGSR	MT, PA	0.853	0.813	0.824	0.637	0.610
Boundary + UGSR	MT, AL	0.885	0.846	0.824	0.670	0.661

AUC, area under the curve; L/S, ratio of the long diameter to the short diameter; PA, pleomorphic adenoma; AL, adenolymphoma; UGSR, ultrasound gray-scale ratio; MT, malignant tumor.

frequency, and scanning depth, can objectively reflect the change of echo intensity in the tumor area to a certain extent.<sup>19</sup> Ultrasonic echo intensity is completely different from the ultrasonic gray scale, but there is a positive correlation between them. Echo intensity ranges from weak to strong, the sound spectrum image from black to white, and the gray value from low to high. The echo intensity of the focus ROI tumor area can be reflected by measuring the gray values on the ultrasound image.<sup>9,10,19</sup> Therefore, the ratio of gray values between the focus areas in the tumor and the surrounding gland in UGSR can meet the need for standardized operating conditions.

In the present study, we found that the L/S value of PA was smaller than that of AL, with the difference bordering on significance, which was consistent with the results reported by Miao et al.<sup>8</sup> L/S is related to the texture and elasticity of the tumor to some extent. A low L/S value indicates that the tumor is less elastic and relatively hard, whereas high L/S values show that the tumor is more elastic and relatively soft. The epithelial and interstitial components of PA, such as cartilage and mucus-like tissue, have complex pathologic structures and are relatively hard, whereas AL contains mostly cystic areas, including epithelial and lymphoid tissues, whose hardness is relatively low. This finding was confirmed by our results.

Reportedly, the hardness of MT is greater than that of benign tumors, and the L/S ratio should be lower in MT than in benign neoplasms. The L/S of MT in this study was slightly higher than that of benign tumors PA and AL, although the differences were not statistically significant. The reason may be that there is some overlap between low-grade malignant tumors and benign tumors, and the L/S value is not suitable for cases in which more than half of the tumor focus areas of the parotid gland are cystic.<sup>8,20,21</sup> However, most of the malignant tumors selected in this study were low-grade lesions, which resulted in a slightly higher L/S ratio in MT than in PA. Follow-up investigations need to collect larger numbers of malignant parotid tumors to explore the differences in L/S between different tumor grades.

We found that the UGSR of MT was significantly higher than that of PA and AL. The UGSR value of PA was larger than that of AL, but the difference was not statistically significant. UGSR is used to distinguish various diseases in the breast and the thyroid and parotid glands.<sup>9,10,22</sup> Chen et al.<sup>10</sup> indicated that UGSR is an objective and quantitative method to evaluate the echo degree of thyroid nodules and has different diagnostic effects for different sizes of nodules.<sup>10</sup> The ROI of the focus selected in our study was the imaging area of the entire tumor. The ratio of the average gray value of the lesion to the average gray value of the

surrounding normal parotid tissue can eliminate the influence of operating factors—such as compensation gain and scanning frequency to some extent—and objectively reflect the change of echo intensity of the diseased tissue.

Yonetsu et al.<sup>23</sup> analyzed the mean gray values and SD of echo intensity of 21 benign parotid tumors and 22 malignant lesions and found that the average gray value of cancer was significantly higher than that of PA and AL, which is consistent with the findings of the present investigation.<sup>23</sup> They also found that the average gray value of PA was significantly higher than that of AL.<sup>23</sup> The relationship between the pathologic tissue and the internal structure of parotid tumors is not clear. Reportedly, most of the weakly hyperechoic structures on ultrasound images consist of connective tissue, zona pellucida, necrosis, and keratinized substances, different contents of which lead to different average gray values. It will be necessary to compare the characteristics of gray ultrasound histograms of the parotid gland with histopathologic patterns to explore the relationship between image features and histology.

We found that tumor boundary, L/S, and UGSR revealed significant differences in values in overall comparisons of the 3 types of tumors. Therefore, ROC analyses were performed for the ability of these parameters, individually and combined, to discriminate between MT, PA, and AL. A commonly used scale for interpretation of AUC states that values of 0.5 to 0.7 indicate poor ability of the test to discriminate between lesions, 0.7 to 0.8 represents acceptable discrimination, 0.8 to 0.9 is excellent, and values > 0.9 are outstanding.<sup>24</sup> The efficacy of L/S in discriminating PA from AL was represented by AUC of 0.698, sensitivity of 0.872, and specificity of 0.500. Although the sensitivity level was good, AUC was approximately 0.7. This result means that L/S values are at best acceptable for distinguishing PA from AL. The use of UGSR alone to distinguish MT from AL (AUC of 0.771) and the combination of L/S and UGSR to discriminate between PA and AL (AUC of 0.741) were found to be acceptable.

However, the diagnostic efficacy of tumor boundary and UGSR together was greatly improved. This combination led to excellent discrimination between MT and PA (AUC = 0.853) and between MT and AL (AUC = 0.885). In both cases, sensitivity and specificity values each exceeded 0.800, which fulfilled the expectation that the sum of these values should exceed 1.5 for tests to be effective.<sup>25</sup>

Some limitations should be noted in our study. The evaluation of each case was retrospective. Also, the tumors themselves existed 3-dimensionally, and the diameter of the long axis was measured on a 2-D image, which could not always show the longest

diameters, so selection bias is inevitable. Despite selecting the focus ROIs over as much of the tumor area as possible, the placement of ROIs was still performed in a manual pattern, which could result in a potential sampling bias. It is hoped that in the future, artificial intelligence technology will help achieve automatic delineation of ROIs to solve this problem. Subtype analysis of histologically different malignant tumors in the parotid gland was not carried out, but the sample size of MTs will be increased in the future, and subgroup analysis will be carried out to improve the value of clinical application.

In conclusion, the morphologic properties of tumor boundary, shape, high rear echo, long and short tumor diameters, L/S, and UGSR differed significantly in various pairwise comparisons of the 3 tumor types. UGSR alone yielded an acceptable distinction between MT and AL. When L/S was combined with UGSR, the AUC value indicated acceptable discrimination between PA and AL. The combination of boundary with UGSR yielded excellent discrimination between MT and PA and between MT and AL. This result suggests a new method for accurate presurgical differential diagnosis of parotid tumors in clinical work without increasing the economic burden to patients.

## DISCLOSURE

None.

## REFERENCES

- Thielker J, Grosheva M, Ihrler S, Wittig A, Guntinas-Lichius O. Contemporary management of benign and malignant parotid tumors. *Front Surg*. 2018;5:39.
- Zhan KY, Khaja SF, Flack AB, Day TA. Benign parotid tumors. *Otolaryngol Clin North Am*. 2016;49:327-342.
- Mansour N, Stock KF, Chaker A, Bas M, Knopf A. Evaluation of parotid gland lesions with standard ultrasound, color duplex sonography, sonoelastography, and acoustic radiation force impulse imaging—a pilot study. *Ultraschall Med*. 2012;33:283-288.
- Psychogios G. Ultrasonography techniques in the preoperative diagnosis of parotid gland tumors—an updated review of the literature. *Med Ultrason*. 2021;23:122-123.
- Bialek EJ, Jakubowski W, Zajkowski P, Szopinski KT, Osmolski A. US of the major salivary glands: anatomy and spatial relationships, pathologic conditions, and pitfalls. *RadioGraphics*. 2006;26:745-763.
- Lee YY, Wong KT, King AD, Ahuja AT. Imaging of salivary gland tumours. *Eur J Radiol*. 2008;66:419-436.
- Gerwel A, Kosik K, Jurkiewicz D. US in preoperative evaluation of parotid gland neoplasms. *Otolaryngol Pol*. 2015;69:27-33.
- Miao LY, Xue H, Ge HY, Wang JR, Jia JW, Cui LG. Differentiation of pleomorphic adenoma and Warthin's tumour of the salivary gland: is long-to-short diameter ratio a useful parameter. *Clin Radiol*. 2015;70:1212-1219.
- Han Z, Lei Z, Li M, Luo D, Ding J. Differential diagnosis value of the ultrasound gray scale ratio for papillary thyroid microcarcinomas and micronodular goiters. *Quant Imaging Med Surg*. 2018;8:507-513.
- Chen X, Gao M, Hu L, Zhu J, Zhang S, Wei X. The diagnostic value of the ultrasound gray scale ratio for different sizes of thyroid nodules. *Cancer Med*. 2019;8:7644-7649.
- Szczypiński PM, Strzelecki M, Materka A, Klepaczko A. MaZda—a software package for image texture analysis. *Comput Methods Programs Biomed*. 2009;94:66-76.
- Kato H, Kanematsu M, Mizuta K, Aoki M. Imaging findings of parapharyngeal space pleomorphic adenoma in comparison with parotid gland pleomorphic adenoma. *Jpn J Radiol*. 2013;31:724-730.
- David E, Cantisani V, De Vincentiis M, et al. Contrast-enhanced ultrasound in the evaluation of parotid gland lesions: an update of the literature. *Ultrasound*. 2016;24:104-110.
- Zajkowski P, Jakubowski W, Bialek EJ, Wysocki M, Osmólski A, Serafin-Król M. Pleomorphic adenoma and adenolymphoma in ultrasonography. *Eur J Ultrasound*. 2000;12:23-29.
- Fodor D, Pop S, Maniu A, Cosgaria M. Gray scale and Doppler ultrasonography of the benign tumors of parotid gland (pleomorphic adenoma and Warthin's tumor). Pictorial essay. *Med Ultrason*. 2010;12:238-244.
- Wu S, Liu G, Chen R, Guan Y. Role of ultrasound in the assessment of benignity and malignancy of parotid masses. *Dentomaxillofac Radiol*. 2012;41:131-135.
- Khalife A, Bakhshae M, Davachi B, Mashhadi L, Khazaeni K. The diagnostic value of B-mode sonography in differentiation of malignant and benign tumors of the parotid gland. *Iran J Otorhinolaryngol*. 2016;28:305-312.
- Nyman HT, Kristensen AT, Skovgaard IM, McEvoy FJ. Characterization of normal and abnormal canine superficial lymph nodes using gray-scale B-mode, color flow mapping, power, and spectral Doppler ultrasonography: a multivariate study. *Vet Radiol Ultrasound*. 2005;46:404-410.
- Roy R, Ghosh S, Ghosh A. Clinical ultrasound image standardization using histogram specification. *Comput Biol Med*. 2020;120:103746.
- Martino M, Fodor D, Fresilli D, et al. Narrative review of multiparametric ultrasound in parotid gland evaluation. *Gland Surg*. 2020;9:2295-2311.
- Hsu JC, Chen PH, Huang KC, Tsai YH, Hsu WH. Efficiency of quantitative echogenicity for investigating supraspinatus tendinopathy by the gray-level histogram of two ultrasound devices. *J Med Ultrason (2001)*. 2017;44:297-303.
- Erol B, Kara T, Gürses C, et al. Gray scale histogram analysis of solid breast lesions with ultrasonography: can lesion echogenicity ratio be used to differentiate the malignancy? *Clin Imaging*. 2013;37:871-875.
- Yonetu K, Ohki M, Kumazawa S, Eida S, Sumi M, Nakamura T. Parotid tumors: differentiation of benign and malignant tumors with quantitative sonographic analyses. *Ultrasound Med Biol*. 2004;30:567-574.
- Hosmer DW, Lemeshow Stanley, Sturdivant RX. *Applied Logistic Regression*. 3rd ed. New York, NY: Wiley; 2013:177.
- Power M, Fell G, Wright M. Principles for high-quality, high-value testing. *Evid Based Med*. 2013;18:5-10.